JOURNAL OF CATALYSIS 112, 93–106 (1988)

Characterization of a Novel K–Co–Mo/Al_2O_3 Water Gas Shift Catalyst

I. Laser Raman and Infrared Studies of Oxidic Precursors

V. KETTMANN,* P. BALGAVÝ,* AND L. SOKOL†

*Department of Analytical Chemistry, Faculty of Pharmacy, Comenius University, 83232 Bratislava, Czechoslovakia; and †Institute for Chemical Utilization of Hydrocarbons, ChZ ČSSP, k.p. Chemopetrol, 43670 Litvínov, Czechoslovakia

Received December 12, 1984; revised August 14, 1987

The oxide form of a novel low-temperature and completely sulfur-tolerant K–Co–Mo/Al_2O_3 catalyst with high activity and selectivity for the WGS reaction has been prepared by a kneading procedure and studied by infrared and Raman spectroscopy. To facilitate the characterization of the catalyst, K/Al_2O_3, Co/Al_2O_3, Mo/Al_2O_3, Co–Mo/Al_2O_3, and K–Co/Al_2O_3 samples prepared under the same conditions have been studied simultaneously. The results on the whole set of samples showed clearly that potassium exerts a major control on the mode of interaction of molybdenum species with the alumina surface. In the absence of potassium, molybdena grows epitaxially on the γ-Al_2O_3 surface and is grouped in heterogeneous clusters which structurally resemble ammonium polymolybdates with varying degrees of aggregation. Removal of NH_4^+ ions due to the addition of K_2CO_3 to Co–Mo/Al_2O_3 leads to the formation of the $K_2Mo_2O_7$ phase probably bound to specific sites of the γ-Al_2O_3 surface. A mechanism is proposed for the $K_2Mo_2O_7$ formation in which surface acidic hydroxyls play an active role. In contrast to molybdenum, cobalt seems to be unaffected by the presence of molybdenum or potassium; the results indicate that cobalt either is dissolved in the γ-Al_2O_3 surface layer or at least selectively blocks octahedral sites of the γ-alumina surface.

INTRODUCTION

As is well known, coal-derived synthesis gas (CO,H_2; $H_2/CO \leq 1$) must be subjected, before utilizing it for synthesis of ammonia, ethanol, or other oxygenates, to hydrodesulfurization (HDS) and water gas shift (WGS) reactions. The latter have been reported to be catalyzed by a number of materials (*1–4*), although iron- and copper-based catalysts are used almost exclusively in industry as WGS catalysts (*5, 6*). Although iron-based catalysts can tolerate small quantities of sulfur, if large-scale conversion of high-sulfur-level coal is to be applied, the relatively large sulfur concentrations found in the syngas would diminish the activity of these catalysts. Thus, completely sulfur-tolerant low-temperature catalyst with high activity and selectivity for the WGS reaction would be desirable. Moreover, if such a catalyst was not only sulfur tolerant but if its activity was even enhanced by sulfur, then single-stage WGS reactors with only one subsequent step to remove CO_2 would be sufficient for pure hydrogen production.

Newsome (*7*) pointed out that K_2CO_3 added to commercial Co–Mo/Al_2O_3 HDS catalyst develops catalytic function for the WGS reaction while maintaining some of the HDS activity. Our studies confirmed that conclusion; in addition, the catalyst was further developed by one of us (L.S.) by optimizing on an empirical basis the catalyst composition and preparation conditions, finally meeting all the above requirements. After a few preparation steps the catalyst is pretreated under quite mild thermal conditions and finally activated by a H_2S/H_2 mixture or directly in the feed stream to the reactor. A number of Czech patents have been granted on these subjects (*8–11*).

0021-9517/88 $3.00

In contrast to Co–Mo/Al_2O_3 HDS catalysts, which have been extensively studied (*12–15*) only a few reports have appeared on the more complex system K–Co–Mo/Al_2O_3 (or K/Al_2O_3, K–Mo/Al_2O_3, etc.). This is rather surprising considering the high industrial importance of the system. Krupay and Amenomiya (*16*) have reported that potassium on alumina weakens the bond between the oxygen and the surface. The effect of KNO_3 (as well as nitrates of other alkali metals) on the nature of molybdenum species supported on γ-Al_2O_3 has been studied by Kordulis *et al.* (*17*). At 673 K all the alkali cations except Li^+ inhibited the reduction of Mo(VI) to Mo(V) and induced a transition from octahedral to tetrahedral coordination symmetry in the Mo(VI) species. The studies of Kantschewa *et al.* (18) on the effect of K_2CO_3 additive on the structural and chemical properties of a conventional Ni–Mo/Al_2O_3 catalyst have led to principally the same conclusion.

In an effort eventually to characterize the industrial K–Co–Mo/Al_2O_3 catalytic system, our research strategy has been first to simplify it by studying the K/Al_2O_3, Co/Al_2O_3, Mo/Al_2O_3, K–Co/Al_2O_3, and Co–Mo/Al_2O_3 systems at various stages during fabrication of the catalyst. By determining what types of metal–support interactions occur in K/Al_2O_3, Co/Al_2O_3, and Mo/Al_2O_3 catalysts, a better understanding of structural and chemical behavior in similar and more complex catalytic systems (i.e., Co–Mo/Al_2O_3, K–Co/Al_2O_3, and finally K–Co–Mo/Al_2O_3) can be gained. We have started with an investigation of the oxidic forms and report here on the structural and physicochemical characteristics of oxide precursors using laser Raman and infrared (IR) spectroscopy.

EXPERIMENTAL

Catalyst preparation. The preparation of catalysts has been described elsewhere (*8–11*). In short, two types of alumina samples were prepared from gibbsite (Žiar nad Hronom, Czechoslovakia): (A) a "precalcined" alumina obtained by heating gibbsite in air at 673 K; (B) microcrystalline boehmite gel prepared by precipitation with formic acid from an alkaline solution (NaOH) of $Al(OH)_3$. The resulting gel was dried in air at 393 K and crushed to fine powder.

The surface area and the pore size distribution of both aluminas were measured using N_2 adsorption at liquid-nitrogen temperature after evacuation of the samples. Alumina A has surface area 170 ± 10 m^2/g and average pore diameter ca. 30 Å; the crystallite size (as determined by X-ray line broadening (*19*)) was 70–80 Å, and the particle size (agglomerates of crystallites) was 0.1–0.2 mm. Alumina B (surface area 200 ± 20 m^2/g) has a bidisperse pore structure, a small fraction of micropores ranging from 10 to 50 Å, and a large fraction of macropores 0.5–1 μm in diameter. X-ray powder diffraction indicated the crystallite size to be <30 Å.

To obtain the resultant support, alumina A and alumina B were mixed together in the weight ratio of 4:1. Catalysts were prepared by mixing weighed amounts of the support and active components ($Co(NO_3)_2 \cdot 6H_2O$, $(NH_4)_2MoO_4$, and/or K_2CO_3) with a small amount of water and mulling into a paste using a kneading machine. The paste was shaped to cylindrical pellets, 6 mm diameter and 10–20 mm long, and finally dried at 393 K prior to use. The catalysts so obtained are designated K/Al_2O_3, Co/Al_2O_3, Mo/Al_2O_3, K–Co/Al_2O_3, Co–Mo/Al_2O_3, K–Co–Mo/Al_2O_3, and Co–Mo–K/Al_2O_3, where the order of active metals represents the order of addition of the respective salts to the kneading mixture. Loadings (expressed as grams of K, Co, or Mo per 100 g of catalyst) were determined from aliquots of the final dried catalysts using atomic absorption spectroscopy, and are K/Al_2O_3, K 10.0; Co/Al_2O_3, Co 1.8; Mo/Al_2O_3, Mo 5.6; Co–Mo/Al_2O_3, Co 1.7, Mo 5.2; K–Co/Al_2O_3, K 9.3, Co 1.5; K–

Co–Mo/Al_2O_3 and Co–Mo–K/Al_2O_3, K 8.4, Co 1.4, Mo 4.4.

Physicochemical Characterization. The Raman spectra were recorded on a JEOL JRS-1 spectrometer, equipped with an argon ion laser (Coherent Radiation 52, 488.0 nm line). The power of the laser, measured at the sample, was 60 mW, and the scan speed varied between 25 and 100 cm^{-1} min^{-1}. The slitwidth was 12 cm^{-1} and the sensitivity was adjusted to the intensity of the Raman signal. The samples were pelletized before and rotated during analysis (40 Hz) to minimize sample heating and/or degradation.

IR spectra were recorded using a Perkin–Elmer 377 dual-beam spectrometer. Disks of 30 mm diameter, weighing 0.40 g, were produced by pressing the samples (2 mg) with dried KBr (0.4 g) as a support material. Attenuation of the reference beam was used to enhance the quality of the spectra and the nominal spectral slitwidth used was typically 4 cm^{-1}. To facilitate the interpretation of the results, IR examination was also performed on samples calcined in air at 723 K.

Powder X-ray diffraction patterns were obtained from the crushed pellets on a Philips PW 1050-25 vertical diffractometer.

DTA measurements were carried out on a DuPont 950 apparatus equipped with high- and medium-temperature cells, using calibrated Pt–10% Rh and Cr–Al thermocouples.

RESULTS AND DISCUSSION

A. Support

As the real industrial K–Co–Mo/Al_2O_3 catalyst operates under a high partial pressure of water vapor, the preparation of the support was chosen so as to minimize the changes in water content during the manufacturing process of the catalyst. On the other hand, the composition of such a support is likely to be of poor reproducibility. In fact, the X-ray diffraction results (not shown here) clearly indicate that during calcination of $Al(OH)_3$ (to prepare alumina A), the solid is not completely dehydrated so that alumina A finally consists of a mixture of $Al(OH)_3$, γ-AlO(OH), and γ-Al_2O_3. Based on the integral intensities of the X-ray lines, the composition of the alumina A used in this particular study was 16 wt% $Al(OH)_3$, 22 wt% γ-AlO(OH), and 62 wt% γ-Al_2O_3. Then, after the mixing of alumina A and alumina B in the 4 : 1 weight ratio, the content of γ-Al_2O_3 in the final support was ca. 50 wt%.

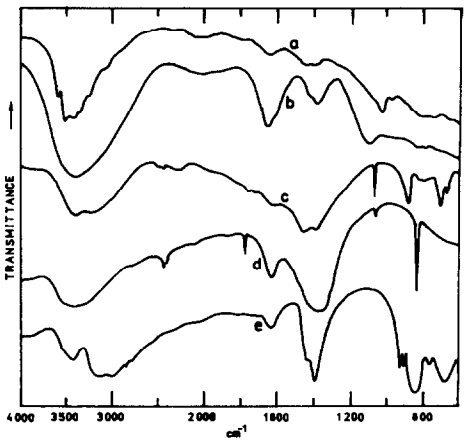

FIG. 1. Infrared transmission spectra of two types of alumina and reference compounds: (a) alumina A, (b) alumina B, (c) K_2CO_3, (d) $Co(NO_3)_2 \cdot 6H_2O$, (e) $(NH_4)_2MoO_4$.

IR spectra of both aluminas (Figs. 1a and b) are dominated by strong and broad absorption bands centered at 3450 and 1640 cm^{-1}, corresponding to stretching and bending frequencies found in the spectrum of liquid water. As revealed from DTA and TG measurements, this water in both aluminas was associated with both adsorbed and capillary-held (in fine micropores) molecular water. The spectrum of Fig. 1a also confirms the presence of gibbsite (bands at 3620, 3520, 3465, 3380, and 1025 cm^{-1}), and boehmite (bands at 3300, 3100, and 1075 cm^{-1}) in alumina A (*20–22*).

B. K/Al_2O_3

To provide a basis for interpretation of the vibrational spectra of the catalysts, we

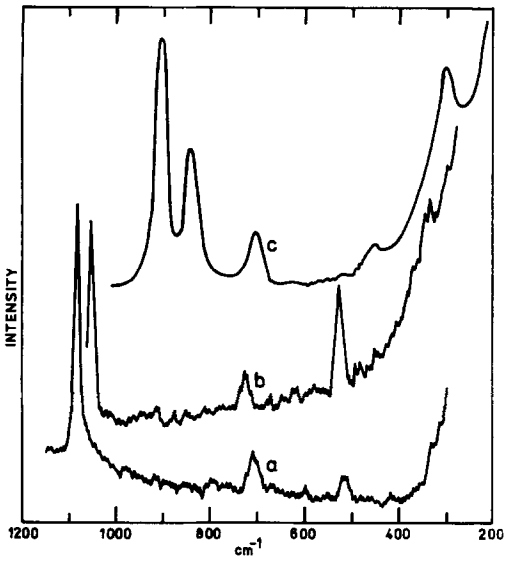

FIG. 2. Raman spectra of reference compounds: (a) K_2CO_3, (b) $Co(NO_3)_2 \cdot 6H_2O$, (c) $(NH_4)_2MoO_4$.

recorded both IR and Raman spectra of the pure compounds used in the catalyst preparation. These are reproduced in Fig. 1 (IR) and Fig. 2 (Raman).

Figure 1c shows the IR spectrum of K_2CO_3; all four normal modes of CO_3^{2-}, $\nu_1(A_1')$, $\nu_2(A_2'')$, $\nu_3(E')$, and $\nu_4(E')$ at 1060, 870, 1410, and 690 cm^{-1}, respectively (*23*), can be seen in the spectrum (the apparent splitting of the 1410 cm^{-1} band together with the presence of the normally forbidden ν_1 band indicates some distortion from D_{3h} symmetry). A comparison with the spectrum of the K/Al_2O_3 sample (Fig. 3b) demonstrates that K_2CO_3 reacted with the surface of the support. The broad band centered at 1410 cm^{-1} was further split into two new strong bands at 1530 and 1410 cm^{-1} formed by the reaction. Another strong band at 1000 cm^{-1} and a band of medium intensity at 3440 cm^{-1} appeared simultaneously, while the 870 cm^{-1} band remained unchanged. Also two weak bands (or shoulders) at 1100 and 1200 cm^{-1} appeared along with the above five bands. Inspection of Fig. 3 (and Fig. 6 presented later) shows that the seven bands were present in the spectra of all samples containing K_2CO_3 and that their absorbance varied in a constant ratio indicating that all these bands belonged to the same species. The 3440 cm^{-1} band is most reasonably an OH stretching mode suggesting that the species contained a hydroxyl group.

In many respects, the IR spectrum in Fig. 3b resembles those reported for CO or CO_2 adsorption on γ-Al_2O_3, K_2CO_3/Al_2O_3, or other oxides (*16, 18, 24–26*). Numerous such studies exist and a number of carbonate and/or bicarbonate (as well as carboxylate) structures have been proposed for the chemisorbed species. Of these, however, the only species containing hydroxyl is a bicarbonate group; for example, Parkyns (*24, 25*) assigned bands at 3605, 1640, 1480, and 1235 cm^{-1} observed for CO_2 adsorption on γ-alumina to, respectively, ν(OH), ν_{as}(CO), ν_{sym}(CO), and δ(COH) modes of a bicarbonate group coordinated in monodentate form to aluminum. Consequently, the assignment of the 1200 cm^{-1} band observed in this study to C–O–H in-plane bending mode is rather straightforward. Similarly, the band at 3440 cm^{-1} is directly attributable to the O–H stretching mode of a bicarbonate; the downward shift in frequency from 3605 cm^{-1} may be caused by hydrogen bonding (the IR studies of Parkyns were conducted at temperatures higher than 673

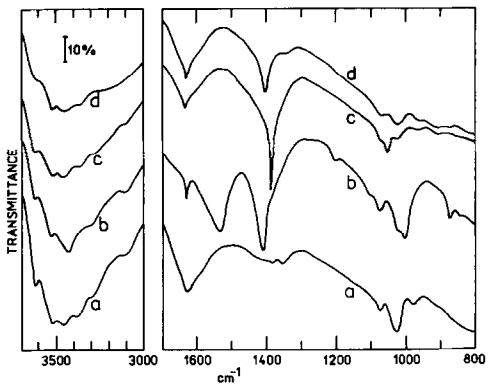

FIG. 3. Infrared transmission spectra of (a) alumina support (4 : 1 mixture of alumina A and alumina B), (b) K/Al_2O_3, (c) Co/Al_2O_3, and (d) Mo/Al_2O_3 after drying at 393 K.

K where one may expect the presence of isolated bicarbonate groups). This was also demonstrated by Bernitt *et al.* (*27*) who observed a band at 3390 cm^{-1} for monomeric (weakly) hydrogen-bonded bicarbonate ions obtained by heating crystalline (dimeric) $KHCO_3$ directly in a KBr matrix. Nevertheless, the displacement of two C–O stretching bands (1530 and 1410 cm^{-1} vs 1640 and 1480 cm^{-1}) was too large to assign them as corresponding modes of monodentate bicarbonate.

The frequencies of these bands, however, are very close to those for the asymmetric and symmetric COO stretching vibrations generally found in the spectra of carboxylates (*23, 28*). This may give a clue to the assignment of the IR bands of the surface species. It is well known that the two COO stretching modes of the carboxylate groups undergo a very small coupling contribution from other vibrations; in contrast, the COO stretching frequencies are highly sensitive to the way in which the carboxylate is coordinated to the metal atom (*28*). Thus, in examining the effect of coordination on the COO stretching frequencies, it is important to interpret the results based on the structures obtained by X-ray analysis. From such studies it can be inferred that the separation between the two stretching frequencies decreases to about 125 cm^{-1} when the carboxylate coordinates in bidentate form to the metal (*29*); for example, bidentate coordination is reported for $Zn(ac)_2 \cdot 2H_2O$ (*30*) and the corresponding separation between the COO stretching frequencies is 95 cm^{-1} (*28*). Thus the 120 cm^{-1} separation observed in this study is in accordance with bidentate behavior of the carboxylate group. These facts led us to conclude that species I must be responsible for the spectrum 3b.

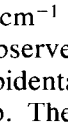

(I)

The position and intensity of the so far unassigned band at 1000 cm^{-1} show that it

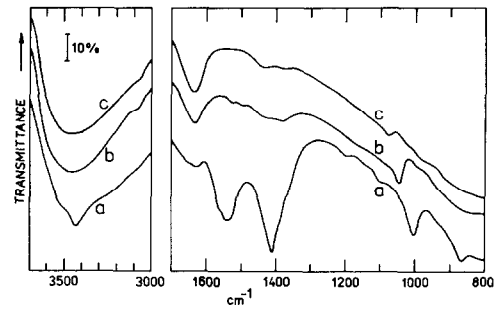

FIG. 4. Infrared transmission spectra of (a) K/Al_2O_3, (b) Co/Al_2O_3, and (c) Mo/Al_2O_3 after calcination at 723 K.

may be due to the C–OH stretching mode. The shoulder at 1100 cm^{-1} is most probably associated with ν_1 vibration of the CO_3 skeleton becoming IR-active since this band was also observed at the same position in the Raman spectrum presented below in Fig. 5a and was thus shifted upward from 1075 cm^{-1} compared to the Raman spectrum of pure K_2CO_3 (Fig. 2a). It is impossible, however, to decide at this stage whether species I is bonded to aluminum or potassium (M = Al or K). The presence of this species even after calcination at 723 K (Fig. 4a) demonstrates its high thermal stability.

In contrast to surface species of adsorbed CO or CO_2 on alumina (or potassium-promoted alumina), only a few studies have appeared up to now in the literature concerning the structures of alkali carbonates on γ-alumina (prepared by the impregnation technique) (*16, 18, 31*). Although these studies did not specify any definite state of potassium, it seems likely that on drying or calcination the surface hydroxyl groups reacted with the carbonate to form OK groups. Although the present results did not reveal the formation of surface K_2O, the following reaction must be envisaged in forming species I:

$$K_2^+CO_3^{2-} + OH^- \rightarrow HCO_3^- + K_2^+O^{2-} \quad (1)$$

The fact that the presence of K_2O has not been detected by X-ray diffraction should be interpreted as meaning that K_2O formed

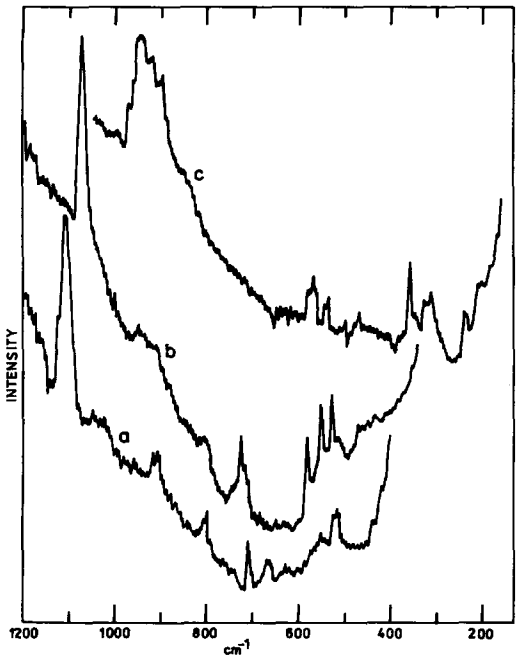

FIG. 5. Raman spectra of (a) K/Al_2O_3, (b) Co/Al_2O_3, and (c) Mo/Al_2O_3 after drying at 393 K.

by reaction (1) did not segregate to form microcrystallites but instead it was well-dispersed over the surface. The loading of K^+ (1.5×10^{21} K^+ ions/g catalyst or 3.7×10^{18} K^+ ions/m^2 γ-Al_2O_3) in our K/Al_2O_3 catalyst was such that one O^{2-} ion per every five OH^- ions was created on the γ-Al_2O_3 surface due to reaction (1). This surface concentration of K_2O was calculated by assuming that K_2CO_3 reacted only with the γ-Al_2O_3 component of the support (50 wt% γ-Al_2O_3, 170 m^2/g) and by using the concentration of 0.93×10^{19} OH^- ions/m^2 γ-Al_2O_3 for the (110) crystal plane of γ-Al_2O_3 which is generally accepted to be preferentially exposed (*32, 33*).

C. Co/Al_2O_3

As shown in Figs. 1d and 2b, pure $Co(NO_3)_2 \cdot 6H_2O$ exhibits two vibrational bands of H_2O (3450 and 1640 cm^{-1}) and three bands at 1385, 825 (IR-active), and 1050 cm^{-1} (Raman-active) which are identified, respectively, with the ν_3, ν_2, and ν_1 normal modes of NO_3^-. The assignment of the relatively intense band at 530 cm^{-1} (Fig. 2b) is less clear and requires some discussion. To our knowledge the Raman spectrum of this compound is not reported in the literature. It is, however, reported that the 450–650 cm^{-1} range is characteristic of wagging vibrations of coordinated water (*28, 34*). Nakagawa and Shimanouchi (*34*) have also carried out normal coordinate analysis on the $[M(H_2O)_6]$ (T_h symmetry) ions and have shown that the H_2O wagging mode belongs to the triply degenerate Raman-active F_g species. As is apparent from Fig. 5b, this band was upon deposition on the support replaced by three bands at 520, 535, and 570 cm^{-1}; i.e., a splitting of the 530 cm^{-1} band of pure $Co(NO_3)_2 \cdot 6H_2O$ occurred. This splitting suggested that a species $[Co(H_2O)_6]^{2+}$ on the catalyst remained intact but became considerably distorted on binding to the surface. Hence, if the interaction with the surface of the support occurred, e.g., through hydrogen bonding, then it had to be substantially stronger than that in bulk $Co(NO_3)_2 \cdot 6H_2O$ (*35*).

Another possibility exists to account for the spectrum in Fig. 5b, namely that the cobalt was incorporated into the γ-Al_2O_3 surface layer (into the octahedral sites as will be discussed later). If this were true, a partially dissociative adsorption of $[Co(H_2O)_6]^{2+}$ would be expected; as a result, cobalt atoms would be surrounded partly by oxygen atoms as well as by water molecules. The occurrence of the well-resolved triplet bands could then be due to the occupation by water molecules of slightly different configurations induced by surface heterogeneity. If this possibility applies, one should observe Raman bands corresponding to Co–O stretching modes at around 690 cm^{-1} as they have been observed, e.g., for Co_3O_4 or α-$CoMoO_4$ on γ-alumina in which Co^{2+} exists, respectively, in distorted tetrahedral or octahedral environments (*36, 37*). The failure to observe a Co–O stretching band in the Raman does not necessarily preclude the existence

of such a species since the band may not have been detected under our experimental conditions (*15, 36*).

Our data alone cannot distinguish between these possibilities; in any case, however, cobalt must be located at the surface. In addition, as the three bands coexist in spectra of all samples containing Co and simply vary in intensity, the highly dispersed nature of the cobalt remains uneffected by the presence of other active metals.

In contrast to cobalt, the symmetry of the NO_3 environment increases on deposition on the support; this is obvious from a comparison of the bandshape of the degenerate $\nu_3(D_{3h})$ vibration at 1385 cm^{-1} in the IR spectra of pure $Co(NO_3)_2 \cdot 6H_2O$ and Co/Al_2O_3 catalyst (Figs. 1d and 3c). The present data do not allow one to determine the nature of this highly symmetrical NO_3^- environment; the calcination of the Co/Al_2O_3 sample at 723 K caused the degradation of the NO_3^-, as shown in Fig. 4b.

D. Mo/Al_2O_3

As shown in Figs. 1e and 2c, the vibrational spectrum of crystalline $(NH_4)_2MoO_4$ exhibits three bands at 900, 845, and 320 cm^{-1} which are identified, respectively, with $\nu_1(A_1)$, $\nu_3(T_2)$, and $\nu_4(T_2)$ modes of MoO_4^{2-} ions (in T_d symmetry); also the IR-active ν_3 and ν_4 modes of tetrahedral NH_4^+ at 3150 and 1400 cm^{-1} in the spectrum 1e are clearly visible (*23*). Comparison of the Raman spectrum 2c with that of Mo/Al_2O_3 catalyst (Fig. 5c) shows that $(NH_4)_2MoO_4$ interacted with the surface of the support. The spectrum in Fig. 5c is dominated by a broad and asymmetric band between 900 and 950 cm^{-1} which is apparently split into at least three distinguishable components with maxima approximately at 945, 920, and 900 cm^{-1}. The broadening of this band indicates that the Mo atoms in Mo/Al_2O_3 sample are not present in a well-defined phase but rather are in slightly different sites presumably in the alumina.

The Raman spectrum of this sample, especially the 900–950 cm^{-1} band, closely resembles those reported by other workers for corresponding Mo/Al_2O_3 catalysts prepared by impregnation in wet, dry, or calcined states (*36–41*); especially a resemblance to wet 8% Mo/Al_2O_3 catalyst prepared by impregnation at pH 11 as reported by Jeziorowski and Knözinger (JK) is remarkable (*38*). Consequently, the Raman spectrum observed in the present study can be interpreted in a similar way. JK interpreted their spectra on the basis of similarity with the spectra of molybdenum–oxygen isopolyanions which are preferentially built up by edge-sharing MoO_6 octahedra and usually give rise to Raman bands in five characteristic frequency regions, namely at 200–250, 300–370, 500–650, 700–850, and 900–1000 cm^{-1}, which are usually assigned, respectively, to Mo–O–Mo deformations, Mo=O bending vibrations, symmetric Mo–O–Mo stretches, asymmetric Mo–O–Mo stretches, and (symmetric and asymmetric) terminal Mo=O stretches. As the position of the bands due to Mo=O stretches in polyanions is proportional to the degree of aggregation, the appearance of at least two bands above 900 cm^{-1} indicates the presence of two octahedral polymeric Mo species differing by the degree of aggregation, while the band at 900 cm^{-1} can already be identified with the ν_1 mode of monomeric tetrahedral MoO_4^{2-}. The major difference between the JK spectra and our spectra involves the low-wavenumber region; contrary to JK, our spectrum contains three pairs of well-resolved bands, one with higher intensity and the other with lower intensity, in the regions characteristic of Mo–O–Mo symmetric stretches, Mo=O bending vibrations, and Mo–O–Mo deformations. Obviously, these bands may be considered as being due to the high-aggregated and low-aggregated octahedral Mo species. Also the ν_4 mode of tetrahedral MoO_4^{2-} clearly appears as a shoulder on the more intense 315 cm^{-1} band.

The surface structure of our Mo/Al_2O_3 catalyst may be most reasonably described

by a combination of the monolayer and patch models which have been reported for related Mo/Al_2O_3 catalysts prepared by impregnation (*42, 43*), i.e., by the patch model, the first layer of 3D patches (clusters) being epitaxial in nature. The arguments for this are presented below.

Judging roughly from the intensities of the Raman bands (Fig. 5c), the ratio of the octahedral to tetrahedral Mo is approximately 3 : 1, which is the ratio of octahedral to tetrahedral cation sites predicted for the preferentially exposed (110) plane of γ-Al_2O_3. Thus the heterogeneous nature and the relative amounts of octahedral and tetrahedral Mo species suggest that the molybdena grows epitaxially on the γ-alumina surface. Stronger evidence for this conclusion is given later (see the discussion on the $Co–Mo/Al_2O_3$ catalyst). By analogy with the impregnated Mo/Al_2O_3 catalysts, formation of such strongly interacted species is expected to involve a reaction with surface OH groups; thus, the following reaction may be considered as a first step in forming the epitaxial layer of molybdena over the γ-alumina:

$$\begin{matrix} -OH^- \\ \\ -OH^- \end{matrix} + (NH_4)_2MoO_4 \rightarrow \left[\begin{matrix} -O \\ \diagdown \\ \quad MoO_2 \\ \diagup \\ -O \end{matrix}\right]^{2-} + 2NH_3 + 2H_2O \quad (2)$$

As noted above, a Raman spectrum quite similar to that in Fig. 5c was obtained by JK for the wet Mo/Al_2O_3 catalyst prepared by "dry" impregnation at pH 11. At this pH tetrahedral MoO_4^{2-} ions predominantly exist in the impregnation solution; i.e., an incorporation of Mo must have taken place by essentially the same mechanism as that depicted in reaction (2). This means that the reaction of MoO_4^{2-} with surface OH groups of γ-Al_2O_3 and subsequent rearrangement of the surface to produce octahedral and tetrahedral Mo interaction species already occur at ambient temperature. Although the Mo loading (3.5×10^{20} Mo atoms/g catalyst) in Mo/Al_2O_3 catalyst is somewhat above the monolayer capacity of the γ-Al_2O_3 present in our support, it is not sufficient to remove all the OH groups expected to be present on the γ-alumina surface even if one assumes that two OH are replaced by each MoO_4^{2-} according to Eq. (2) and that an OH concentration of 0.93×10^{19} OH groups/m^2 γ-Al_2O_3 is considered (the surface concentration of OH groups should be even higher for the γ-Al_2O_3 immersed in H_2O). In spite of this, some amount of NH_4^+ ions is still present in the catalyst as shown in Fig. 3d where both IR-active modes of NH_4^+ are clearly visible. This might indicate that Mo grows as a monolayer in small patches until a certain portion of the γ-Al_2O_3 surface is covered. Existing Mo patches could induce changes in the γ-Al_2O_3 surface properties so that further amounts of Mo interact with the patches rather than with the free portion of the surface. Two layers which are formed by reaction (2) and terminate the spinel lattice appear to serve as a matrix in forming the multilayers; i.e., clusters of octahedral Mo are formed over the aggregated Mo placed in the octahedral sites of the first epitaxial layer; similarly, once a tetrahedral site in the alumina surface layer is occupied by Mo, multilayers will also contain tetrahedrally coordinated Mo. Thus, NH_4^+ ions are in multilayers of the clusters perdominantly associated with the tetrahedral Mo as some portion of the NH_4^+ is removed during the aggregation to form the octahedral Mo:

$$y(NH_4)_2MoO_4 \rightarrow (NH_4)_{2y-x}Mo_yO_{4y-x/2} + x/2H_2O \quad (3)$$

where y is the degree of aggregation.

E. Co–Mo/Al₂O₃

The spectra are presented in Figs. 6, 7, and 8. Addition of molybdenum to Co/Al_2O_3 (cobalt in our Co-containing catalysts was always introduced prior to molybdenum) resulted in dramatic differences in the

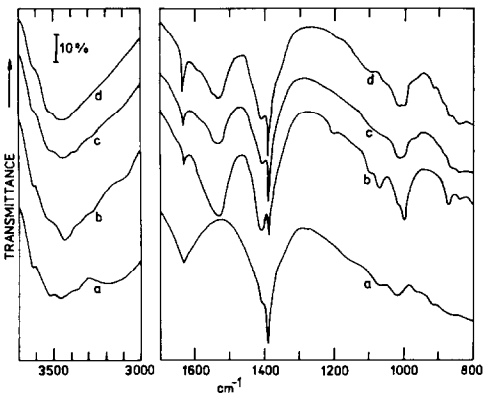

FIG. 6. Infrared transmission spectra of (a) Co–Mo/Al_2O_3, (b) K–Co/Al_2O_3, (c) K–Co–Mo/Al_2O_3, and (d) Co–Mo–K/Al_2O_3 after drying at 393 K.

vibrational spectra, as indicated in Figs. 6a and 8b. From a comparison of the Raman spectra of Mo/Al_2O_3 and Co–Mo/Al_2O_3 catalysts (Figs. 5c and 8b) it is obvious that the two bands at 920 and 900 cm^{-1} present in Mo/Al_2O_3 disappeared and were replaced by a band at 907 cm^{-1}. The position of this band is intermediate between the assignments to low-aggregated octahedral Mo and monomeric tetrahedral MoO_4^{2-} and a simple assignment of this band to either would not be fully correct. Since, however, the band about 320 cm^{-1} (attributable to the ν_4 vibration of MoO_4^{2-}) is clearly visible and has considerably enhanced intensity compared to that in Mo/Al_2O_3, it can be concluded that the 907 cm^{-1} band is due to the ν_1 vibration of monomeric tetrahedral molybdates. A similar upward shift in the frequency of the ν_1 stretching mode was recently also observed by Kantschewa *et al.* (*18*) and was attributed to distortion of tetrahedral symmetry due to bonding to the surface. Considerable changes also occur in the 300 to 600 cm^{-1} region of the Raman spectrum. In addition to the enhanced intensity of the 320 cm^{-1} band, most striking is the disappearance of three pairs of bands which were present in the spectrum of Mo/Al_2O_3 (a pair of bands at 540 and 575 cm^{-1} would have been obscured by the Co triplet bands but the other pairs are clearly absent) indicating the presence of the aggregated Mo species in too low a concentration to give rise to Mo–O–Mo low-wavenumber bands at a detectable level. In other words, monomeric tetrahedral Mo appears to grow at the expense of the polymeric species. This trend toward partial destruction of polymolybdate species is consistent with the data of Fig. 6a where the enhanced IR intensity of NH_4^+ bands at 1400 cm^{-1} (this

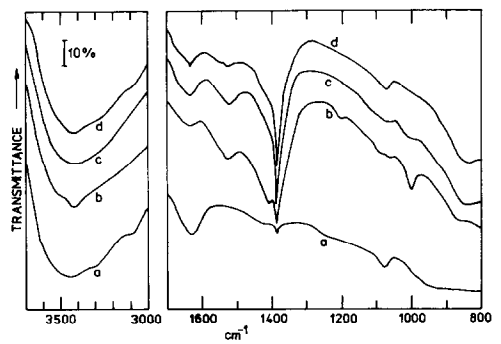

FIG. 7. Infrared transmission spectra of (a) Co–Mo/Al_2O_3, (b) K–Co/Al_2O_3, (c) K–Co–Mo/Al_2O_3, and (d) Co–Mo–K/Al_2O_3 after calcination at 723 K.

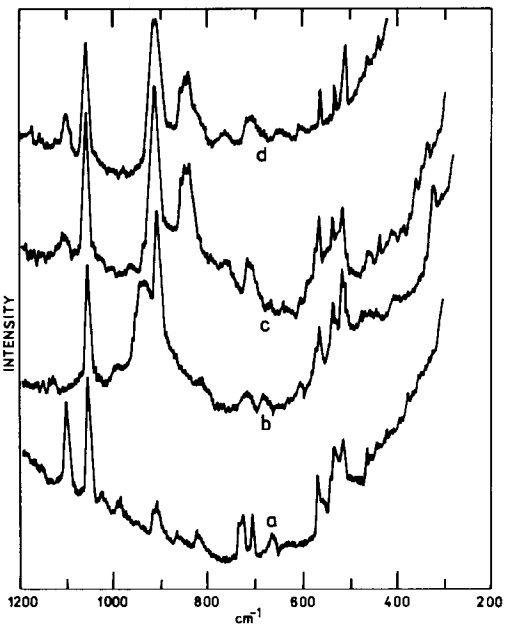

FIG. 8. Raman spectra of (a) K–Co/Al_2O_3, (b) Co–Mo/Al_2O_3, (c) K–Co–Mo/Al_2O_3, and (d) Co–Mo–K/Al_2O_3 after drying at 393 K.

band appears as a shoulder on the more intense "nitrate" band) and the 3000 to 3300 cm^{-1} region compared to Mo/Al_2O_3 sample implies in accordance with Eq. (3) an increased percentage of the monomeric molybdates. Only a negligible amount of NO_3^- in the calcined $Co–Mo/Al_2O_3$ sample, producing a weak residual ν_3 band (Fig. 7a), shows that NH_4^+ ions were really associated (similarly to that in Mo/Al_2O_3 sample) with the molybdates rather than with NH_4NO_3 or NH_4NO_3-like species.

The Raman spectrum of our $Co–Mo/Al_2O_3$ catalyst matches no known spectra of Mo compounds (the trivial possibility that the $Co–Mo/Al_2O_3$ sample is a simple mixture of polymeric molybdates and unreacted $(NH_4)_2MoO_4$ may be ruled out because of the shifting of the ν_1 band and absence of the ν_2 band at about 845 cm^{-1}) nor of any well-defined Co–Mo phases reported, e.g., for the corresponding impregnated and calcined catalytsts. For instance, both α- and β-$CoMoO_4$, the latter being structurally equivalent to the Co–Mo "bilayer" (*44*), should give rise to major bands at about 960 and 690 cm^{-1}.

As noted above, cobalt is not notably affected by the presence of molybdenum, as shown by comparison of Figs. 5b and 8b. This as well as other experimental results described above led us to conclude that cobalt interacts strongly with the γ-Al_2O_3 surface rather than with molybdenum. The nature of the interaction must be such that cobalt preferentially occupies octahedral sites in the epitaxial layer on the γ-Al_2O_3 surface or essentially intact $[Co(H_2O)_6]^{2+}$ ions selectively interact with specific sites on the γ-alumina surface, ultimately blocking the formation of octahedral polymolybdates. Indeed, simple calculations, using the Knözinger–Ratnasamy model of γ-Al_2O_3 (*33*) and again assuming that (110) planes predominantly terminate the γ-Al_2O_3 crystallites, show that about 78% of the octahedral sites in the first epitaxial layer of the γ-Al_2O_3 surface for this particular support is blocked (or occupied) by the Co loading (1.7×10^{20} Co atoms/g catalyst) in our $Co–Mo/Al_2O_3$ catalyst. Remaining octahedral sites may be occupied by 0.9 wt% Mo and surface tetrahedral sites can accommodate 1.2 wt% Mo. A predominance of tetrahedral over octahedral Mo is consistent with the Raman intensities (Fig. 8b) but only 2.1 wt% Mo is required to cover the surface epitaxial layer of γ-Al_2O_3. A comparison with the total Mo loading (5.2 wt%) shows that multilayers of Mo species must have been formed even if a uniform coverage of the γ-Al_2O_3 surface is presumed. The Mo phase, however, is most probably akin to that in Mo/Al_2O_3 catalyst, clustered into small disordered three-dimensional patches leaving some portions of the γ-Al_2O_3 surface uncovered.

F. K–Co/Al₂O₃

As shown in Figs. 6b and 8a, the vibrational spectrum of the $K–Co/Al_2O_3$ sample may well be described as a superposition of the spectra of K/Al_2O_3 and Co/Al_2O_3 samples. This demonstrates that the nature of the species present in K/Al_2O_3 and Co/Al_2O_3 samples are not mutually influenced when deposited simultaneously on the support surface, the only exceptions being the NO_3^- and HCO_3^- ions. Although the shape of the ν_3 band of NO_3^- at 1385 cm^{-1} in $K–Co/Al_2O_3$ is very similar to that in Co/Al_2O_3, the band in the former sample remained, in contrast to the latter sample, completely unaffected after the calcination (Fig. 7b). This suggests that NO_3^- ions in $K–Co/Al_2O_3$ exist in an environment different from that of the Co/Al_2O_3. The sharpness of the ν_3 band precludes the existence of NO_3^- in the bulk-like low-temperature KNO_3 phase (aragonite structure) (*23, 28*). Although the similarity of the observed spectrum in Fig. 6b to that of the calcite-type phase I of KNO_3 is much better, considering the high dispersion of potassium it is more likely that NO_3^- ions are also well dispersed due to the bonding to the surface at the K^+ sites. The precise nature of the highly symmetrical NO_3^- environment can-

not be revealed from the data presented here. From a comparison of the spectra in Figs. 6b and 7b it is further apparent that calcination caused the bicarbonate bands to be reduced in intensity while the nitrate band persists at the original intensity. These observations may be explained by considering that NO_3^- ions compete with HCO_3^- for exposed K^+ sites, bonding of NO_3^- being more stable. This again implies the surface nature of potassium.

G. K–Co–Mo/Al_2O_3 and Co–Mo–K/Al_2O_3

Addition of molybdenum to K–Co/Al_2O_3 or of potassium to Co–Mo/Al_2O_3 samples resulted in several significant changes in both the IR and the Raman spectra, as can be seen in Figs. 6 and 8. IR spectra of Figs. 6c and 6d revealed that the bands due to HCO_3^- were considerably reduced in intensity (to ~55% of their original intensity as estimated from the absorbance of the 1530 cm^{-1} band), while the broad absorbance corresponding to the stretching vibration of NH_4^+ ions completely disappeared (the absence of the ν_4 band of NH_4^+ at 1400 cm^{-1} could not be verified since this spectral region was masked by the bicarbonate and nitrate bands). Considerable changes occur in the Raman spectra (Fig. 8c and 8d). In addition to the diminished intensity of the ν_1 band of bicarbonates at 1100 cm^{-1}, most striking is the appearance of new broad bands centered at 850 cm^{-1} (this band is apparently split into three components) and 710 cm^{-1}, while the 945 and 325 cm^{-1} bands (present in the spectrum of Co–Mo/Al_2O_3) have completely disappeared. The signal-to-noise ratio also permitted the detection of numerous weak bans in the 300 to 500 cm^{-1} region which appeared simultaneously with the above two bands (Fig. 8c), while the most prominent band at 907 cm^{-1} was broadened and shifted slightly to ~910 cm^{-1}.

Recalling that these spectral features were not observed in any samples discussed above, one might suggest that the species giving rise to these bands contained molybdenum and potassium. Indeed, the positions and relative intensities of these bands were in excellent agreement with those of $K_2Mo_2O_7$ (*45*) (taking into account removal of NH_4^+ ions, the presence of isomorphous $(NH_4)_2Mo_2O_7$ with essentially identical Raman spectrum (*46*) had to be excluded). Especially the occurrence of the most intense band at ~910 cm^{-1} and the absence of a band at 325 cm^{-1} are a conclusive indication for the existence of $K_2Mo_2O_7$ since such spectral features are characteristic of no other spectra of Mo compounds. A major difference between the spectrum of this supported species and that of bulk $K_2Mo_2O_7$ is the larger width of the bands (especially those of the Co–Mo–K/Al_2O_3 sample); these observations can be accounted for by the heterogeneous nature of the γ-alumina surface and hence by distortions of the coordination polyhedra on the surface. Thus, the preparation technique used in this work leads to a catalyst with a surface structure entirely different from that of K–Ni–Mo/Al_2O_3 catalyst prepared by impregnation with K_2CO_3 of a conventional Ni–Mo/Al_2O_3 catalyst for which the formation of surface K_2MoO_4 has been proposed (*18*).

Our Raman and IR data are therefore consistent with the following sequence of reactions:

$$2(NH_4)_2MoO_4 + 2K_2CO_3 \rightarrow 4NH_3 + 2CO_2 + 2H_2O + 4K^+ + 2MoO_4^{2-} \quad (4a)$$

$$2MoO_4^{2-} + 2OH^- \rightarrow 2HMoO_4^- + 2O^{2-} \quad (4b)$$

$$2HMoO_4^- \rightarrow Mo_2O_7^{2-} + H_2O \quad (4c)$$

$$Mo_2O_7^{2-} + 2O^{2-} + 4K^+ + H_2O \rightarrow K_2Mo_2O_7 + K_2O + 2OH^- \quad (4d)$$

The structure of $K_2Mo_2O_7$ has been reported to consist of infinite chains of $Mo_2O_7^{2-}$ ions, the chains comprising pairs of edge-shared distorted MoO_6 octahedra, and

having adjacent pairs linked by distorted MoO_4 tetrahedra. Each chain comprises an equal number of MoO_4 and MoO_6 units, and potassium ions occupy interchain positions. This structure observed by X-ray analysis is thus equivalent to one of those predicted by Tytko (*49*) on the basis of theoretical considerations. This author has also presented evidence that the polycondensation of MoO_4^{2-} ions to form bulk dimolybdate chains is possible only in the presence of protons, e.g., from NH_4^+ of $(NH_4)_2MoO_4$. As the NH_4^+ ions in our K–Co–Mo/Al_2O_3 (or Co–Mo–K/Al_2O_3) catalyst were stoichiometrically driven off by the reaction with K_2CO_3, the only possible source of protons necessary for MoO_4^{2-} protonation appears to be surface acidic hydroxyls of the alumina support (Eq. (4b)). The hydroxyl groups are then regenerated at the end of the reaction sequence. Thus it may be possible that the ease of formation of $K_2Mo_2O_7$ is related to the acidity of the support and that the condensation mainly proceeds through direct hydrogenation of MoO_4^{2-} adsorbed on acidic sites of the support. It is, however, not clear from our results whether or not these acidic sites are identical with or related to those involved in reaction (*1*).

The fact that the K–Co–Mo/Al_2O_3 and Co–Mo–K/Al_2O catalysts gave the same vibrational spectra (Figs. 6 and 8) means that in the presence of potassium the reaction (4a) is thermodynamically more favorable than reaction (1) as well as reaction (2), the latter leading to dissolution of Mo^{6+} in the surface layer of the γ-alumina. It also shows indirectly that reactions (4a) through (4d) have already proceeded at room temperature during the kneading procedure. The present results, however, cannot reveal whether the observed $K_2Mo_2O_7$ phase is attached to the support surface or whether it is present as a separate phase. However, an epitaxial growth of $K_2Mo_2O_7$ in small patches (chains) is possible over the γ-Al_2O_3 surface; there are no crystallographic arguments against a dissolution of Mo^{6+} ions in a surface C-layer (using the notation originally prescribed by Lippens and de Boer (*32*)) of the (110) plane of γ-Al_2O_3 to form very short isolated chains of $Mo_2O_7^{2-}$ (of type D according to Tytko (*49*)) consisting of a pair of edge-shared MoO_6 octahedra and two pairs of MoO_4 tetrahedral linked via corner-sharing to the octahedra. It therefore may well be possible that in the presence of K_2CO_3, molybdenum interacts strongly not only with potassium but also with specific sites on the γ-Al_2O_3 surface, ultimately forming very small clusters of $K_2Mo_2O_7$ epitaxially bound to the γ-alumina surface. The observed heterogeneous character of $K_2Mo_2O_7$ supports this possibility.

Further insight into the surface structure of our K–Co–Mo/Al_2O_3 and Co–Mo–K/Al_2O_3 catalysts can be obtained from simple stoichiometric considerations. The metal loadings in our catalysts correspond to a Co : Mo : K atomic ratio of approximately 1 : 2 : 9. Thus, if 1 mol of Co is taken as a reference, all of the 2 mol of $(NH_4)_2MoO_4$ is converted via reactions (4a)–(4d) to the surface $K_2Mo_2O_7$. The remaining 2.5 mol of K_2CO_3 then reacts via reaction (1) analogously to that in K/Al_2O_3 to produce bidentate bicarbonate coordinated to K^+ sites of highly dispersed K_2O. As mentioned above, the nature of cobalt is unaffected by the presence of other active components. A further diminution of the IR intensity of the biacarbonate bands upon calcination (Figs. 7c and 7d) can again be explained by the competitive mechanism described above.

CONCLUSIONS

We have reached the following conclusions as a result of this physicochemical and structural investigation of the K–Co–Mo/Al_2O_3 WGS and related (K/Al_2O_3, Co/Al_2O_3, Mo/Al_2O_3, Co–MO/Al_2O_3, and K–Co/Al_2O_3) catalysts prepared by kneading of the active salts with the support.

1. The Al_2O_3 support is a complex mixture of $Al(OH)_3$, γ-AlO(OH), and γ-Al_2O_3

and thus contains a wide spectrum of structural, physisorbed, and capillary water.

2. Based on the IR results a mechanism was postulated for K_2CO_3 interaction over γ-Al_2O_3 in which CO_3^{2-} interacts with surface hydroxyl to form a bicarbonate group coordinated in bidentate form to K^+ ions which are well dispersed on the γ-Al_2O_3 surface as a 2D K_2O-like structure.

3. Mo ions in Mo/Al_2O_3 catalyst are grouped in cluster arrangements, bound epitaxially to the γ-alumina. Various (at least three) types of clusters exist; a majority of the clusters consists of octahedral Mo species with structures analogous to those of ammonium polymolybdates with varying degrees of aggregation. Also a small fraction of clusters containing bulk-like $(NH_4)_2MoO_4$ exists. The relative amounts of the octahedral and tetrahedral Mo species appear to be related to the epitaxial character of the cluster-γ-Al_2O_3 interfacial layer and to the randomness in filling the cationic sites of this layer by molybdenum. Such a surface structure appears to be a general characteristic of Mo/Al_2O_3 catalysts prepared by OH^-–MoO_4^{2-} ion-exchange adsorption. Although the adsorption most probably preferentially occurs at basic OH groups, the subsequent dissolution of Mo^{6+} in the γ-Al_2O_3 surface layer occurs with essentially no site preference.

4. Our Raman results are compatible with the view that cobalt, in marked contrast to molybdenum, preferentially occupies or selectively blocks the octahedral sites in the surface epitaxial layer of γ-Al_2O_3. This strong metal–support interaction in the Co/Al_2O_3 system appears to be unaffected by the presence of other catalytically active components. We consider that the ultimate consequence of a strong preference for octahedral sites by cobalt is an increased percentage of tetrahedral molybdates (analogous to bulk $(NH_4)_2MoO_4$) in the Co–Mo/Al_2O_3 sample.

5. The final industrial WGS K–Co–Mo/Al_2O_3 catalyst exhibits not only physicochemical and structural properties characteristic of the related simpler systems (K/Al_2O_3, etc.) but also certain specific characteristics. Part of the K_2CO_3 reacts rapidly with $(NH_4)_2MoO_4$ leaving behind potassium. Complete removal of NH_4^+ ions and the presence of K^+ cause the molybdenum to interact with the potassium and probably also with the γ-Al_2O_3 surface forming oriented (epitaxially bound) clusters of the $K_2Mo_2O_7$ phase which was strongly indicated by the Raman spectroscopy. A mechanism was postulated for $K_2Mo_2O_7$ formation in which surface acidic hydroxyls acted as the hydrogen source.

ACKNOWLEDGMENTS

We are pleased to thank Dr. M. Kotouček and Dr. J. Pisarčík for recording the IR and Raman spectra.

REFERENCES

1. Taylor, K. C., Sinkevitch, R. M., and Klimisch, R. L., *J. Catal.* **25,** 44 (1974).
2. Grenoble, D. C., Estadt, M. M., and Ollis, D. F., *J. Catal.* **67,** 90 (1981).
3. Sato, S., and White, J. M., *J. Catal.* **69,** 128 (1981).
4. Hou, P., Meeker, D., and Wise, H., *J. Catal.* **80,** 280 (1983).
5. Brunauer, L., and Keenan, A., *J. Amer. Chem. Soc.* **64,** 751 (1942); Bohlbro, H., *J. Catal.* **3,** 207 (1964).
6. Sengupta, G., Gupta, D. K., and Sen, S. P., *Indian J. Chem. Sect. A* **16,** 1030 (1978).
7. Newsome, D. S., *Catal. Rev. Sci. Eng.* **21,** 275 (1980).
8. Sokol, L., Czech. patent 199187.
9. Sokol, L., Koleník, Š., and Horyna, V., Czech. Patent 215515.
10. Sokol, L., *Ropa Uhlie* **34,** 10, 587 (1982).
11. Sokol, L., Domalíp, V., Brzobohatý, P., and Loukota, J., Czech. Patent 214610.
12. Massoth, F. E., *J. Catal.* **36,** 164 (1975); **47,** 316 (1977).
13. deBeer, V. R. J., Beverlander, C., van Sint Fiet, T. H. M., Werter, P. G. A., and Amberg, C. H., *J. Catal.* **43,** 68 (1976); de Beer, V. H. J., van der Aalst, M. J. M., Machiels, C. J., and Schuit, G. C. A., *J. Catal.* **43,** 78 (1976).
14. Hagenbach, G., Courty, P., and Delmon, B., *J. Catal.* **31,** 264 (1973); Delmon, B., "The Chemistry and Uses of Molybdenum" (H. F. Barry, and P. C. H. Mitchell, Eds.), p. 73. Climax Molybdenum Co., Ann Arbor, MI 1979.
15. Wivel, C., Clausen, B. S., Candia, R., Mørup, S.,

and Topsøe, H., *J. Catal.* **87,** 497 (1984); Topsøe, H., and Clausen, B. S., *Catal. Rev. Sci. Eng.* **26,** 395 (1984); Derouane, E. G., Pedersen, E., Clausen, B. S., Gabelica, Z., Candia, R., and Topsøe, H., *J. Catal.* **99,** 253 (1986).
16. Krupay, B. W., and Amenomiya, Y., *J. Catal.* **67,** 362 (1981).
17. Kordulis, C., Violotis, S., and Lycourghiotis, A., *J. Less-Common Met.* **84,** 197 (1982).
18. Kantschewa, M., Delannay, F., Jeziorowski, H., Delgado, E., Eder, S., Ertl, G., and Knözinger, H., *J. Catal.* **87,** 482 (1984).
19. McVicker, G. B., and Vannice, M. A., *J. Catal.* **63,** 25 (1980).
20. Shcherban, S. A., and Nurmagambetov, K. N., *Zh. Prikl. Spektrosk.* **13,** 566 (1970).
21. Rouquerol, J., Fraissard, J., Mathieu, M.-V., Elston, J., and Imelik, B., *Bull. Soc. Chim. Fr.* **12,** 4233 (1970).
22. Wickersheim, K. A., and Korpi, G. K., *J. Chem. Phys.* **42,** 579 (1965).
23. Ross, S. D., "Inorganic Infrared and Raman Spectra." McGraw–Hill, London, 1972.
24. Parkyns, N. D., *J. Chem. Soc. A,* 410 (1969).
25. Parkyns, N. D., *J. Phys. Chem.* **75,** 526 (1971).
26. He, M.-Y., and Ekerdt, J. G., *J. Catal.* **87,** 381 (1984).
27. Bernitt, D. L., Hartmann, K. D., and Hisatsune, I. C., *J. Chem. Phys.* **42,** 3553 (1965).
28. Nakamoto, K., "Infrared Spectra of Inorganic and Coordination Compounds." Wiley, New York, 1970.
29. Battiston, G., and Sbrignadello, G., *Inorg. Chim. Acta* **26,** 145 (1978).
30. Talbot, J. H., *Acta Crystallogr.* **6,** 720 (1953).
31. Stork, W. H., and Pott, G. T., *J. Phys. Chem.* **78,** 2496 (1974).
32. Lippens, B. C., and De Boer, J. H., *Acta Crystallogr.* **71,** 1312 (1964).
33. Knözinger, H., and Ratnasamy, P., *Catal. Rev. Sci. Eng.* **17,** 31 (1978).
34. Nakagawa, I., and Shimanouchi, T., *Spectrochim. Acta* **20,** 429 (1964).
35. Prelesnik, B. V., Gabela, F., Ribár, B., and Kostanovič, I., *Cryst. Struct. Commun.* **2,** 581 (1973).
36. Medema, J., van Stam., de Beer, V. H. J., Konings, A. J. A., and Koningsberger, D. C., *J. Catal.* **53,** 386 (1978).
37. Cheng, C. P., and Schrader, G. L., *J. Catal.* **60,** 276 (1979).
38. Jeziorowski, H., and Knözinger, H., *J. Phys. Chem.* **83,** 1166 (1979).
39. Brown, F. R., Makovsky, L. E., and Rhee, K. H., *J. Catal.* **50,** 162, 385 (1977).
40. Wang L., and Hall, W. K., *J. Catal.* **66,** 251 (1980).
41. Zingg, D. S., Makovsky, L. E., Tischer, R. E., Brown, F. R., and Hercules, D. M., *J. Phys. Chem.* **84,** 2898 (1980).
42. Schuit, G. C. A., and Gates, B. C., *AIChE J.* **19,** 417 (1973).
43. Schrader, G. L., and Cheng, C. P., *J. Catal.* **80,** 369 (1983).
44. Gajardo, P., Grange, P., and Delmon, B., *J. Catal.* **63,** 201 (1980).
45. Becher, H. J., *Z. Anorg. Allg. Chem.* **474,** 63 (1981).
46. Tytko, K.-H., and Schönfeld, B., *Z. Naturforsch. B* **30,** 471 (1975).
47. Magarill, S. A., and Klevtsova, F. F. *Sov. Phys. Crystallogr.* **16,** 645 (1972).
48. Armour, A. W., Drew, M. G. B., and Mitchell, P. C. H., *J. Chem. Soc. Dalton Trans.,* 1493 (1975).
49. Tytko, K.-H., *Z. Naturforsch. B* **31,** 737 (1976).